

Analysis of power transformer

Transient analysis of power transformer using FEM

ABSTRACT

The article presents the coupled finite element method (FEM) with circuit equations used for analysis of transformers. The magnetic field and the voltages on windings are coupled together and solved. Three different types of transformers in 2D and 3D were simulated in harmonic case and transient case. The results of currents and voltages on windings are provided. In addition, the magnetic field is displayed. The transient response of three-phase power transformer is simulated for the case of unbalanced loadings and the case of one opened loading. Numerical results demonstrate that the simulation tool with FEM method provides a quick, efficient and reliable way to analyze transformers.

KEYWORDS

FEM, transient field, nonlinear, coupled field-circuit, transformer, inrush currents

1. Introduction

A transformer is a piece of electrical equipment that transfers electric energy between two or more circuits through coils by electromagnetic induction. A varying current in the transformer's primary winding creates a varying magnetic flux in the core producing a varying electromotive force (EMF) or voltage in the secondary winding. How to accurately and efficiently predict the currents and voltages on the primary winding and the secondary winding is a challenging problem, especially for cores with nonlinear material properties. Numerical modelling techniques for Maxwell's equations, such as FEM, enable analysis of all important phenomena occurring inside the transformers and exterior to them. This includes the currents and voltages in the windings, the magnetic saturation of the materials, and the generation of heat by the coils and the transformer core losses. In this article, firstly, the coupled field-circuit equation based on Maxwell equation and circuit equation with finite element method in 2D and 3D is presented. Secondly, the scheme of solving transient

FEM modelling enables analysis of transformer internal and external phenomena, including winding currents and voltages, material magnetic saturation, heat generation, and core losses

nonlinear field-circuit coupled model with Newton-Raphson method is outlined. Finally, a simply one-phase transformer, a step-up autotransformer and a delta-to-star three-phase power transformer with different loadings were simulated by Oersted 9.3 in 2D and Faraday 9.3 in 3D.

2. Electromagnetic field equation for a transformer

The fundamental equation governing the electromagnetic field in a transformer with the stranded windings can be expressed by magnetic vector potential \vec{A} and electric scalar potential V [1]

$$\nabla \times (\mu^{-1} \nabla \times \vec{A}) + \sigma \frac{\partial \vec{A}}{\partial t} + \sigma \nabla V = \sum_{k=1}^N \vec{J}_k \quad (1)$$

$$\vec{J}_k = I_k \frac{n_k}{S_k} \hat{l}_k = J_k \hat{l}_k \quad (1a)$$

where:

μ is the magnetic permeability,

σ is the electric conductivity,

n_k is the number of coil turns,

S_k is the cross section, and

\hat{l}_k is a unit tangential direction of the k -th winding coil.

I_k is the current on the coil to be determined.

In the two-dimensional model where the geometry and material quantities are independent of one axis, for example, z-axis, the governing equation can be simplified by

$$\nabla \times (\mu^{-1} \nabla \times (A\hat{z})) + \sigma \frac{\partial (A\hat{z})}{\partial t} = \sum_{k=1}^N J_k \hat{z} \quad (1b)$$

After space discretization of (1b) with the proper boundary condition using Galerkin's method [2], the following matrix is derived

$$[K]\tilde{A} + [M] \frac{d\tilde{A}}{dt} - [D]I = 0 \quad (2)$$

where:

$$[K] = \{ \langle \nabla \times \vec{w}_j, (\mu^{-1} \nabla \times \vec{w}_i) \rangle \}, [M] = \{ \sigma \langle \vec{w}_j, \vec{w}_i \rangle \}, [D] = \{ \langle \vec{w}_j, \hat{l}_k \frac{n_k}{S_k} \rangle \},$$

$$A = \sum A_i N_i(x, y), \tilde{A} = (A_1, A_2, \dots, A_M)^T, I = (I_1, I_2, \dots, I_N)^T, \text{ and}$$

$N_i(x, y)$ is a shape function associated with the node.

For the three-dimensional case, the edge-based basis $\vec{w}_i(\vec{r})$ as a tangential shape function [3] associated with the edge can be chosen and the matrix $[K]$, $[M]$ and $[D]$ can be expressed by

$$[K] = \{ \langle \nabla \times \vec{w}_j, (\mu^{-1} \nabla \times \vec{w}_i) \rangle \}, [M] = \{ \sigma \langle \vec{w}_j, \vec{w}_i \rangle \}, [D] = \{ \langle \vec{w}_j, \hat{l}_k \frac{n_k}{S_k} \rangle \} \quad (3)$$

3. External circuit equation

Due to the connection of windings in transformers to the external voltage sources or external loadings, there exists the relationship among the flux linkages, currents in the coils and external input voltages or loadings. This relationship is expressed with the equation based on Kirchhoff's current law and Kirchhoff's voltage law.

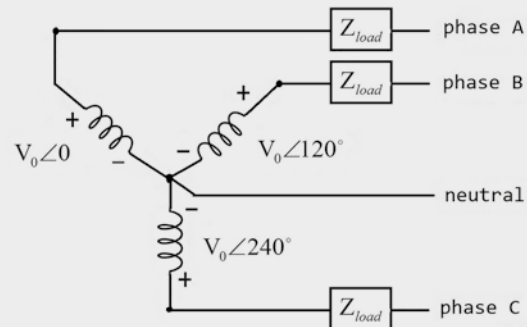


Figure 1. Three-phase Y-connection winding with the balanced loading

As an example for the three-phase Y-connection winding with the balanced loading shown in Fig.1, the equations are expressed by

$$V_p = (R_{load} + R_p^{coil})I_p(t) + L_{load} \frac{d}{dt} I_p(t) + C_{load}^{-1} \int I_p(t) dt + \frac{d}{dt} \Phi_p^{coil}(t) \quad (4)$$

$$p = A, B, C$$

$$I_A(t) + I_B(t) + I_C(t) = 0 \quad (4a)$$

where:

V_p is the input source voltage,

R_{load} is the resistance,

L_{load} is inductance, and

C_{load} capacitance of the loading,

R_p^{coil} is the resistor of the coil, and

$\Phi_p^{coil}(t)$ is the flux linkage on the coil, which can be represented by:

Due to connections of windings to external voltage sources or loads, there exists the relationship among the flux linkages, currents in the coils and external input voltages or loads

$$\Phi_p^{\text{coil}}(t) = \frac{N_p}{S_p} \frac{\partial}{\partial t} \int \hat{l}_p \cdot \vec{A}(\vec{r}, t) dV \quad (4b)$$

The circuit equation (2) is coupled with the quantity of the magnetic vector potential \vec{A} in the field equation.

The equation of the currents on the winding can be written as

$$V_0(t) \begin{pmatrix} \angle 0 \\ \angle 120 \\ \angle 240 \end{pmatrix} = \begin{pmatrix} D_A & 0 & 0 \\ 0 & D_B & 0 \\ 1 & 1 & D_C + 1 \end{pmatrix} \begin{pmatrix} I_A \\ I_B \\ I_C \end{pmatrix} + \frac{d}{dt} \begin{pmatrix} N_A S_A^{-1} \int \hat{l}_A \cdot \vec{A}(\vec{r}, t) dV \\ N_B S_B^{-1} \int \hat{l}_B \cdot \vec{A}(\vec{r}, t) dV \\ N_C S_C^{-1} \int \hat{l}_C \cdot \vec{A}(\vec{r}, t) dV \end{pmatrix} \quad (5)$$

where $D_p = R_{\text{load}} + R_p^{\text{coil}} + L_{\text{load}} \frac{d}{dt} + C_{\text{load}}^{-1} \int \cdot dt$.

For the general case of transformers, the circuit equation is the following form [4]:

$$[E] \frac{d\vec{A}}{dt} + [R]I + [L] \frac{dI}{dt} + [C] \int_0^t I(t) dt = V(t) \quad (6)$$

where:

- [R] is the matrix related to the resistances on the loadings and the resistors on the coils,
- [L] and [C] are the matrix related to the inductances and capacitances on the loadings, and
- [E] is the magnetic flux in the coils.

4. The scheme of transient nonlinear field-circuit coupled model

In order to solve the time-dependent system of equations (2) and (6), a numerical integration scheme with T time step is expressed by

$$\begin{aligned} \theta[K] \vec{A}^{n+1} + (1-\theta)[K] \vec{A}^n + T^{-1}[M](\vec{A}^{n+1} - \vec{A}^n) \\ - [D](\theta I^{n+1} + (1-\theta)I^n) = 0 \end{aligned} \quad (7)$$

$$\begin{aligned} [E]T^{-1}(\vec{A}^{n+1} - \vec{A}^n) + [R](\theta I^{n+1} + (1-\theta)I^n) + [L]T^{-1}(I^{n+1} - I^n) \\ + \frac{1}{2}T[C]I^{n+1} + T[C] \sum_{i=1}^n I^i = (\theta V^{n+1} + (1-\theta)V^n) \end{aligned}$$

where the value of θ parameter determines the time-stepping scheme, such as Euler Backward or Crank-Nicholson algorithm.

The compact forms of the above scheme can be written as

$$\begin{aligned} \begin{pmatrix} \theta[K] + T^{-1}[M] & -[D]\theta \\ [E]\theta & T\theta\{[R]\theta + [L]T^{-1} + \frac{1}{2}T[C]\} \end{pmatrix} \begin{pmatrix} \vec{A}^{n+1} \\ I^{n+1} \end{pmatrix} \\ = \begin{pmatrix} -(1-\theta)[K] & [D](1-\theta) \\ [E]\theta & T\theta\{-[R](1-\theta) + [L]T^{-1}\} \end{pmatrix} \begin{pmatrix} \vec{A}^n \\ I^n \end{pmatrix} \\ + \begin{pmatrix} 0 \\ T\theta\{(\theta V^{n+1} + (1-\theta)V^n) - T[C] \sum_{i=1}^n I^i \} \end{pmatrix} \Rightarrow \begin{pmatrix} f^n \\ g^n \end{pmatrix} \end{aligned} \quad (8)$$

When the magnetic permeability μ of the core material is non-linear, the classical Newton-Rasphson method is utilized to solve the following equation:

$$\begin{pmatrix} \theta[K] + T^{-1}[M] & -[D]\theta \\ [E]\theta & T\theta\{[R]\theta + [L]T^{-1} + \frac{1}{2}T[C]\} \end{pmatrix} \begin{pmatrix} \vec{A}^{n+1} \\ I^{n+1} \end{pmatrix} = \begin{pmatrix} f^n \\ g^n \end{pmatrix}$$

Set $\begin{pmatrix} \vec{A}^{n+1} \\ I^{n+1} \end{pmatrix}^0 = \begin{pmatrix} \vec{A}^n \\ I^n \end{pmatrix}$ and (9)

$$\begin{aligned} - \begin{pmatrix} \theta[K(A^n)] + T^{-1}[M] & -[D]\theta \\ [E]\theta & T\theta\{[R]\theta + [L]T^{-1} + \frac{1}{2}T[C]\} \end{pmatrix} \\ \begin{pmatrix} \vec{A}^n \\ I^n \end{pmatrix} + \begin{pmatrix} f^n \\ g^n \end{pmatrix} \Rightarrow \begin{pmatrix} \Delta f^n \\ \Delta g^n \end{pmatrix} \end{aligned}$$

And solve the equation:

$$\begin{aligned} \begin{pmatrix} \theta[\partial K] + T^{-1}[M] & -[D]\theta \\ [E]\theta & T\theta\{[R]\theta + [L]T^{-1} + \frac{1}{2}T[C]\} \end{pmatrix} \begin{pmatrix} \Delta \vec{A}^{n+1} \\ \Delta I^{n+1} \end{pmatrix} \\ = \begin{pmatrix} \Delta f^n \\ \Delta g^n \end{pmatrix} \end{aligned} \quad (10)$$

where:

$$[\partial K] = \{ \langle \nabla N_j, ((dH/dB)^{-1} \nabla N_i) \rangle \}$$
 for 2D, and

$$[\partial K] = \{ \langle \nabla \times \vec{w}_j, ((dH/dB)^{-1} \nabla \times \vec{w}_i) \rangle \}$$
 for 3D.

The input power and output power of the transformer are calculated by:

$$P_{\text{input}} = \sum_i |I_i^{\text{source}} V_i^{\text{source}}| \quad (11a)$$

$$P_{\text{output}} = \sum_i |I_i^{\text{load}} V_i^{\text{load}}| \quad (11b)$$

For the harmonica case at the operation frequency ω , the coupled circuit-field equation will be

$$\begin{pmatrix} [K] + j\omega[M] & -[D] \\ j\omega[E] & [R] + j\omega[L] + (j\omega)^{-1}[C] \end{pmatrix} \begin{pmatrix} \vec{A} \\ I \end{pmatrix} = \begin{pmatrix} 0 \\ V(\omega) \end{pmatrix} \quad (12)$$

5. Application examples and discussions

In order to validate the proposed procedure, three different types of transformers with 2D and 3D models were simulated based on the above procedures. All of simulations were performed on a personal computer with Intel(R) Core™ i7-4930 CPU @ 3.40 GHz and 64 GB RAM.

A) A single phase transformer

First, a simple small one-phase 120 V / 12 V transformer with M19 silicon steel non-linear material core operated at the frequency 60 Hz is considered.

Table 1. The specification of a one-phase transformer

Core size	2.5 x 21.77 cm ²
Window size	1.625 x 5.24 cm ²
Thickness	3.17 cm
Primary coil	450 turns / 2.4 Ω
Primary coil size	0.5 x 2.01 cm ²
Secondary coil	50 turns / 0.0296 Ω
Secondary coil size	0.5 x 2.01 cm ²
Input voltage	120 V
Loading resistance	0.533 Ω
Loading inductance	1 mH
Loading capacitance	1 mF

The geometrical models in 2D and 3D are shown in Fig. 2.

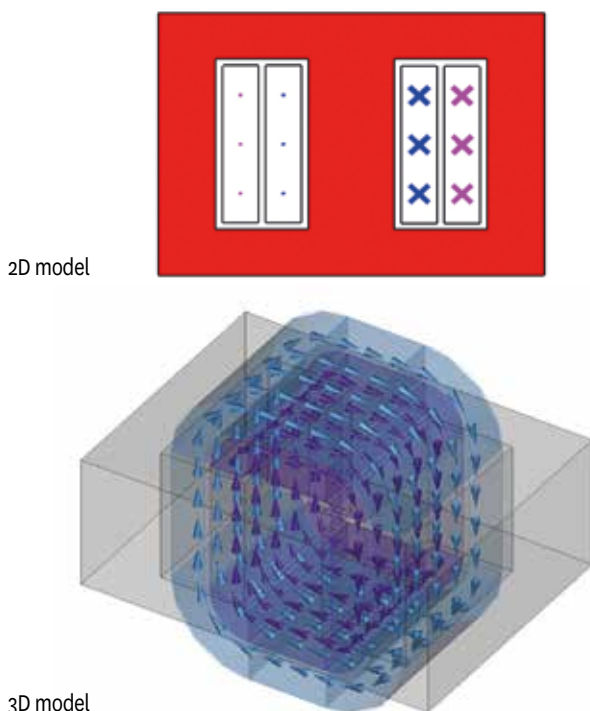


Figure 2. The geometrical models in 2D and 3D

”In order to validate the proposed procedure, three different types of transformers with 2D and 3D models were simulated on a personal computer

For the transient input voltage source $V(t)=120\sin(\omega t)$ (V) on the primary winding, the currents on input port and output port vs. the time are plotted in Fig. 3.

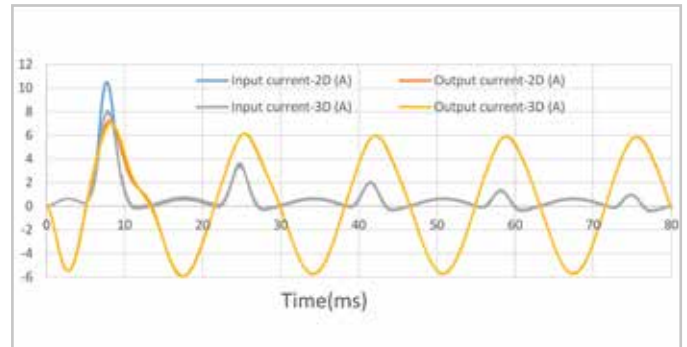


Figure 3. Input current on the primary winding and output current on the secondary winding

From Fig. 3, the inrush currents on the primary coil obtained by the 2D and 3D methods are very similar except the first peak.

The magnetic flux density inside the core at the second peak time ($t=0.025$ s) of the inrush currents in 2D and 3D is plotted in Fig. 4.

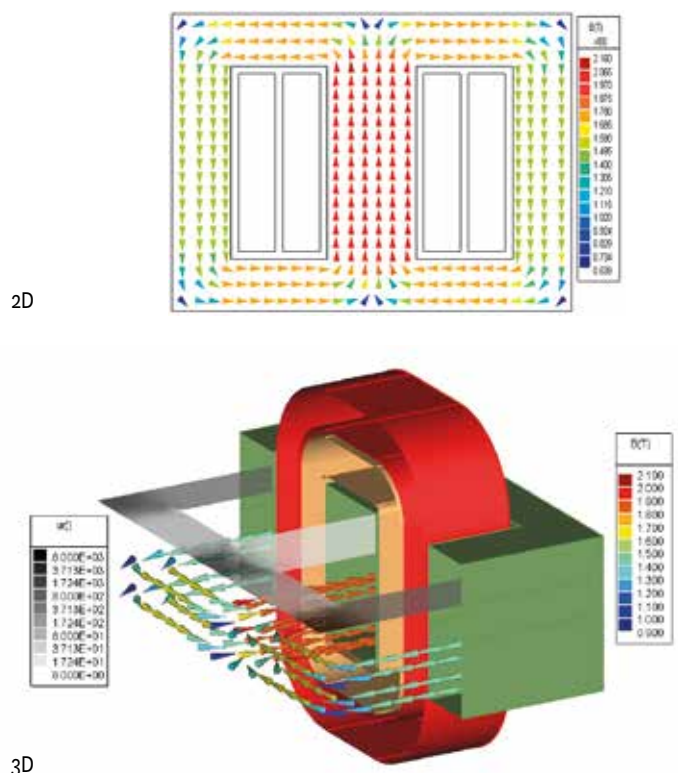


Figure 4. Magnetic flux density inside core at the time 0.025 s in 2D and 3D

”High-magnitude inrush currents, generated when transformer cores are driven into saturation during energization, have undesirable effects, including potential damage of the transformer, and reduced power quality on the system

Transformer inrush currents are high-magnitude currents generated when transformer cores are driven into saturation during energization. These currents have undesirable effects, including potential damage to or loss-of-life of the transformer, and reduced power quality on the system. Therefore, inrush current prediction is an important issue during transformer design. Transient simulation provides a good approach to analysis of the inrush currents.

The running time of the 2D model with 13667 triangular elements and 27350 unknowns is 41 minutes and 8 seconds. The running time of the 3D model with 89291 tetrahedral elements and 104111 unknowns is 2 hours and 33 minutes.

B) Step-up autotransformer

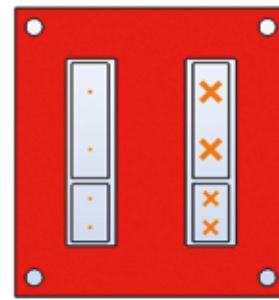
An autotransformer is a special electrical transformer having part of its winding included in both input and output circuits. In an autotransformer, portions of the winding serve as both the primary and secondary sides of the transformer. Their biggest advantage is the reduction of size, weight and cost compared with the general isolated transformer. Table 2 is the specification of a 105 V / 120 V, 250 W step-up autotransformer at 60 Hz operating frequency with M19 silicon steel non-linear material core, which is based on the reference [5].

Table 2. The specification of a step-up autotransformer

Core size	2.5 x 15.16 cm ²
Window size	1.625 x 2.82 cm ²
Thickness	3.17 cm
Boost coil	69 turns / 0.17 Ω
Boost coil size	0.5 x 2.01 cm ²
Main coil	459 turns / 5.75 Ω
Main coil size	1.0 x 2.01 cm ²
Input voltage	105 V
Output voltage	120 V
Output current	2.08 A
Output power	250 W
Output load	57.69 Ω

The geometrical models in 2D and 3D are shown in Fig. 5.

2D geometry



3D geometry

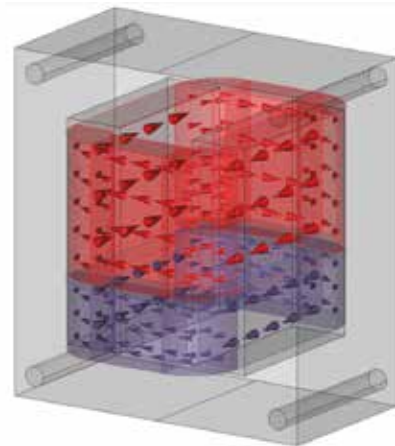


Figure 5. The geometrical models in 2D and 3D

The results at the frequency 60 Hz in 2D and in 3D are listed in Table 3 on page 70.

For the transient input voltage source $V(t)=120\sin(\omega t)$ (V) on the primary winding, the currents on input port and output port vs. the time are plotted in Fig. 3.

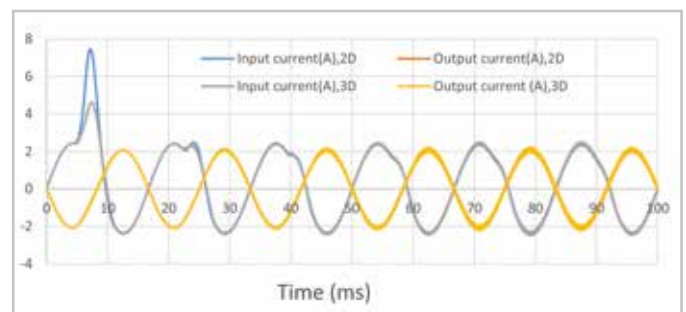


Figure 6. The transient response of input current and output current in 2D and 3D model

From Fig. 5 and 6, the simulation results from 2D and 3D codes are very similar in the late-time period except the first peak. The inrush current on the input port in 2D is more than twice that of the ordinary input current.

The magnetic flux density inside the core at the first peak time 0.0071 s of the inrush currents is shown in Fig. 7.

”A 105 V / 120 V, 250 W step-up autotransformer at 60 Hz operating frequency with M19 silicon steel non-linear material core was also analysed

Table 3. The result of voltage, current, winding turn loss, input power and output power

Quantity	2D model	3D model
Input voltage (V)	105 \angle -5.4E-16	105 \angle -3.041E-07
Output voltage (V)	120.1 \angle 179.8	120.1 \angle 179.7
Input current (A)	2.396 \angle -1.240	2.395 \angle 179.8
Output current (A)	2.082 \angle 179.8	2.082 \angle 179.7
Winding turn loss (W)	1.3088	1.306
Real input power (W)	251.495	251.454
Real output power (W)	250.186	250.148

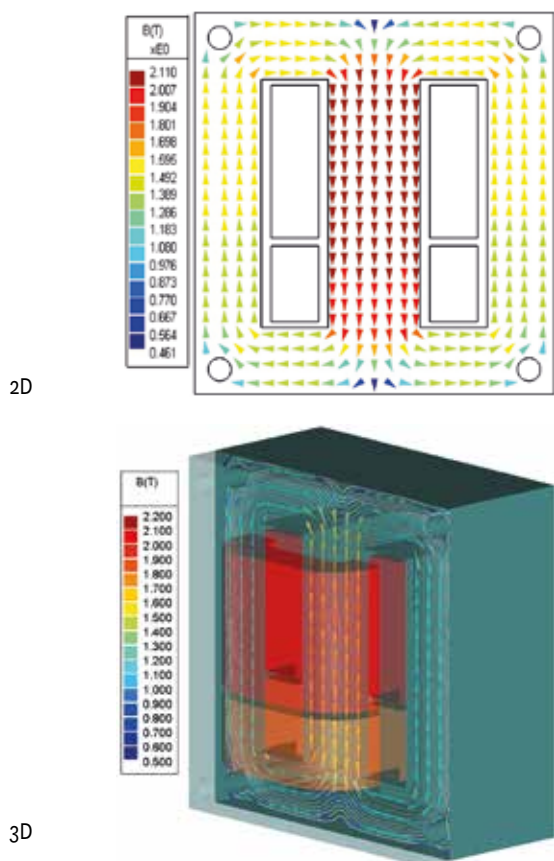


Figure 7. The magnetic flux density inside the core at the time 0.0071 s

The running time of the 2D model with 14649 triangular elements and 29334 unknowns is 23 minutes and 2 seconds. The running time of the 3D model with 89291 tetrahedral elements and 53826 unknowns is 1 hours 3 minutes and 38 seconds.

C) Three-phase three-limb delta-to-star transformer

Finally, an 11 kV / 110 kV three-phase three-limb delta-to-star transformer, which is used in most of power systems, is considered. The specification of the transformer from the reference [6] is shown in Table 4. Compared with previous transformers, this transformer is large in size.

” FEM method can catch peaks of inrush currents, allowing engineers to understand the phenomenon of over-saturation in transformers

Table 4. The specification of a three-phase three-limb delta-to-star transformer

Core size	2.82 x 2.97 m ²
Window size	1.37 x 0.6 m ²
Thickness	0.5 m
Low Volt coil	83 turns / 0.057 Ω
Low Volt coil size	1.162 x 0.1 m ²
High Volt coil	860 turns / 1.33 Ω
High Volt coil size	1.162 x 0.14 m ²
Distance from low volt coil to limb and high volt coil	0.02 m
Core diameter	0.54 m
Input voltage	11 kV
Output voltage	110 kV
Output load	500 Ω

The geometrical model in 2D and 3D is shown in Fig. 8.

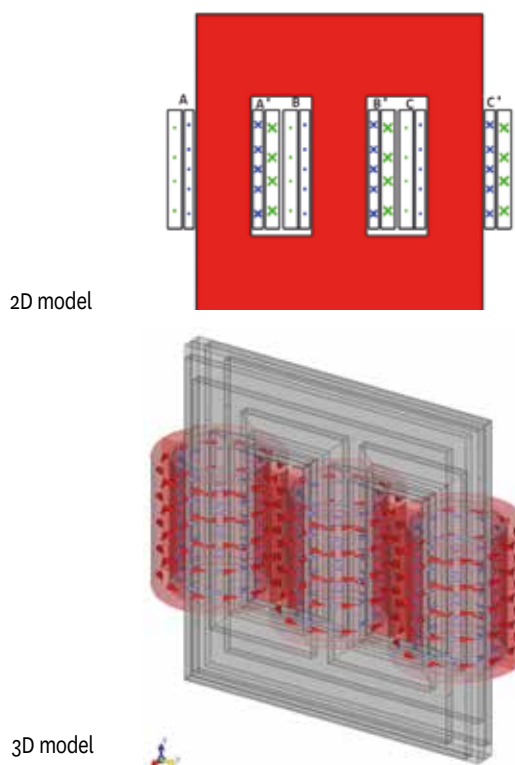


Figure 8. The geometrical model in 2D and 3D

The results at the frequency 60 Hz simulated with Oersted (2D) and Faraday (3D) are listed in Table 5.

For the transient input voltage source on the low voltage winding $V_0(\sin(\omega t), \sin(\omega t + \frac{2}{3}\pi), \sin(\omega t + \frac{4}{3}\pi))$, the currents on the input port vs. the time steps are plotted in Fig. 9.

Table 5. The result of voltages, currents, winding turn loss, input power and output power

Quantity	2D model	3D model
Voltage on low volt coil-A (kV)	11.0 \angle -89.96	11.0 \angle -90.0
Voltage on low volt coil-B (kV)	11.0 \angle 30.0	11.0 \angle 30.0
Voltage on low volt coil-C (kV)	11.0 \angle 150.0	11.0 \angle 150.0
Voltage on high volt coil-A (kV)	112.1 \angle -92.64	111.28 \angle -96.48
Voltage on high volt coil-B (kV)	111.2 \angle 27.41	111.36 \angle 23.5
Voltage on high volt coil-C (kV)	112.3 \angle 147.4	111.41 \angle 143.5
Current on low volt coil-A (kA)	2.336 \angle -93.94	2.307 \angle -96.85
Current on low volt coil-B (kA)	2.310 \angle 26.47	2.297 \angle 23.33
Current on low volt coil-C (kA)	2.331 \angle 146.8	2.307 \angle 143.5
Current on high volt coil-A (kA)	0.2242 \angle 87.35	0.2226 \angle 83.52
Current on high volt coil-B (kA)	0.2244 \angle -152.6	0.2227 \angle -156.5
Current on high volt coil-C (kA)	0.2243 \angle -32.62	0.2228 \angle -36.48
Turn loss on low volt coils (MW)	0.9273	0.9102
Turn loss on high volt coils (MW)	0.2008	0.1979
Real input power (MW)	76.60	75.50
Real output power (MW)	75.47	74.40

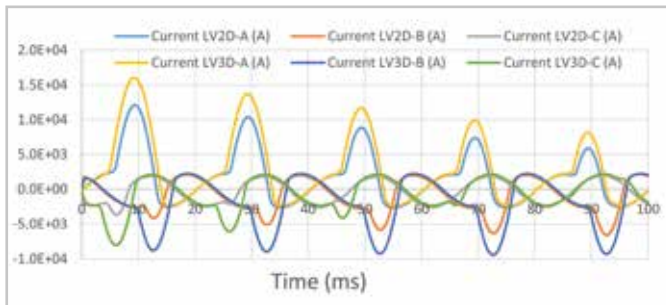


Figure 9. The three-phase currents on LV windings in 2D and 3D models

For the unbalanced load (500, 525 550) Ω and (∞ , 500 500) Ω (opened on the first phase) on three phases in the 2D model, the currents on the input port vs. the time steps are plotted in Fig. 10.

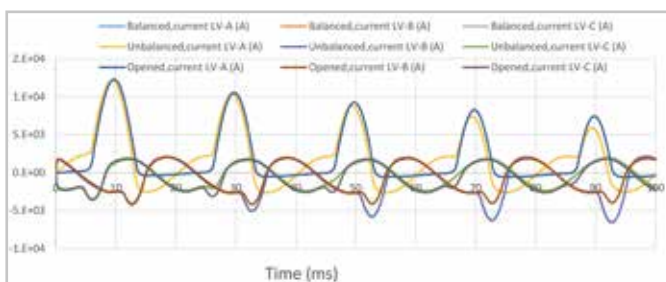


Figure 10. Three phase currents on LV windings in 2D

6. Conclusion

The simulation results for the different types of transformers performed in 2D and 3D show that the simulation tool using the FEM method provides a quick and efficient way to analyze transformers. The method can catch the peaks of inrush currents, allowing engineers to understand the phenomenon of over-saturation in transformers.

The thermal distributions (temperature) within the transformer and supporting structures can be subsequently calculated using the losses determined by the FEM electromagnetic solution. These losses would be the input for a FEM thermal solution. The description of this process is left for a future article.

Bibliography

- [1] T. Renyuan, W. Shenghui, L. Yan, W. Xiulian, C. Xiang: "Transient simulation of power transformers using 3D finite element model coupled to electric circuit equations", IEEE Trans. Mag., 2000, 36 (4), pp. 1417–1420.
- [2] M. V. K. Chari and S. J. Salon, Numerical Methods in Electromagnetism, New York, Academic, 2000.
- [3] J.P. Webb. Hierarchical vector basis functions of arbitrary order for triangular and tetrahedral finite elements. IEEE Transactions on Antennas and Propagation, 47(8):1495–1498, August 1999.
- [4] J.-S. Wang, "A nodal analysis approach for 2D and 3D magnetic-circuit coupled problems," IEEE Trans. Mag., Vol. 32, No. 3, pp. 1074–1077, May 1996.
- [5] C.W.T. McLyman, "Designing a step-up autotransformer", Kg Magnetics, Inc., P.O. Box 3703, Idyllwild, CA29549-3703.
- [6] T.H. Fawzi, A. Abd Elkhalek, „New approaches for the applications of FEM in the routine design of power transformers using PCs“, 18th International Conference on Electricity Distribution Turin, 6-9 June 2005.

Authors



Bruce Klimpke obtained his M.Sc. degree in electrical engineering from the University of Manitoba in 1984. Since then he has been the Technical Director at Enginia Research Inc. During this time Mr. Klimpke has worked on the development of the boundary element method and the finite element method as applied to electromagnetic problems.



Chaowei Su obtained the M.Sc. degree in applied mathematics from Northwestern Polytechnical University in 1986. Since 2002, he has been a R&D scientist at Enginia Research Inc. His major field is numerical computation of electromagnetic fields.